

Technique for the Dry Transfer of Epitaxial Graphene onto Arbitrary Substrates

Joshua D. Caldwell,^{†,*} Travis J. Anderson,[†] James C. Culbertson,[†] Glenn G. Jernigan,[†] Karl D. Hobart,[†] Fritz J. Kub,[†] Marko J. Tadjer,[†] Joseph L. Tedesco,[†] Jennifer K. Hite,[†] Michael A. Mastro,[†] Rachael L. Myers-Ward,[†] Charles R. Eddy, Jr.,[†] Paul M. Campbell,[†] and D. Kurt Gaskill[†]

[†]U.S. Naval Research Laboratory, 4555 Overlook Avenue, S.W., Washington, D.C. 20375 and [†]Electrical Engineering Department, University of Maryland, College Park, Maryland 20742

ABSTRACT To make graphene technologically viable, the transfer of graphene films to substrates appropriate for specific applications is required. We demonstrate the dry transfer of epitaxial graphene (EG) from the C-face of 4H-SiC onto SiO₂, GaN and Al₂O₃ substrates using a thermal release tape. Subsequent Hall effect measurements illustrated that minimal degradation in the carrier mobility was induced following the transfer process in lithographically patterned devices. Correspondingly, a large drop in the carrier concentration was observed following the transfer process, supporting the notion that a gradient in the carrier density is present in C-face EG, with lower values being observed in layers further removed from the SiC interface. X-ray photoemission spectra collected from EG films attached to the transfer tape revealed the presence of atomic Si within the EG layers, which may indicate the identity of the unknown intrinsic dopant in EG. Finally, this transfer process is shown to enable EG films amenable for use in device fabrication on arbitrary substrates and films that are deemed most beneficial to carrier transport, as flexible electronic devices or optically transparent contacts.

KEYWORDS: epitaxial graphene · transfer · silicon intercalation · Hall effect · transparent contact · SiC

Reports of single layer graphene have drawn significant interest due to its exciting properties, such as ballistic carrier transport,^{1,2} high thermal and electrical conductivity, optical transmission,^{3–5} and high mechanical hardness.⁶ Films used in those studies were created primarily *via* the exfoliation method,^{1,5} which produces small-area flakes with variable size, shape, and thickness. To use graphene as a conductive, optically transparent contact, the reproducible transfer of large-area graphene films that can subsequently be patterned into top-side contacts is required. For use in device fabrication, the impact of carrier scattering from the underlying substrates that dramatically influences the carrier behavior of graphene-based devices must be taken into account.^{7–9} Konar *et al.*⁹ recently reported that while high- κ dielectric materials aid carrier transport in graphene by minimizing the impact of Coulombic and impurity scattering of charged

carriers, these improvements are reduced or offset due to surface-optical phonon scattering of the carriers from polar lattice vibrations within the dielectric medium. Therefore, transfer of device quality EG films onto materials with both a high dielectric constant and high surface-optical phonon energies, such as AlN, is also desired. Furthermore, the transfer of graphene onto SiO₂ and Si are desired to enable easier integration into current electronic circuitry. Such large-area graphene films can be produced by either metal-catalyzed growth on films of nickel^{10–12} or copper¹³ or by epitaxial growth through the sublimation of silicon from the surface of silicon carbide (SiC).^{14–19} Epitaxial graphene (EG) films grown on the carbon-terminated surface of SiC have been shown to be of high quality, with room temperature Hall mobilities up to 4200 cm²/(V s) having been observed in 16 mm × 16 mm C-face EG films grown within our lab.²⁰ Furthermore, we have observed room temperature Hall effect mobilities as high as 27000 cm²/(V s) from specific 10 μm Hall crosses fabricated on C-face grown EG films. However, the C-face films, while exhibiting significantly higher mobilities than those grown on the Si-face, do tend to have a high variability in the EG film thickness across a given sample.

Here we present results illustrating a dry transfer technique using Nitto Denko Revalpha thermal release tape that has enabled the transfer of large areas (squares up to 16 mm on a side) of EG from the C-face SiC “donor” substrate onto various “handle” substrates, with C-face grown EG material chosen due to its promising electrical properties. Successful transfers of C-face EG onto SiO₂ on Si, GaN, and Al₂O₃ films depos-

*Address correspondence to Joshua.caldwell@nrl.navy.mil.

Received for review November 9, 2009 and accepted January 12, 2010.

Published online January 25, 2010. 10.1021/nn901585p

© 2010 American Chemical Society

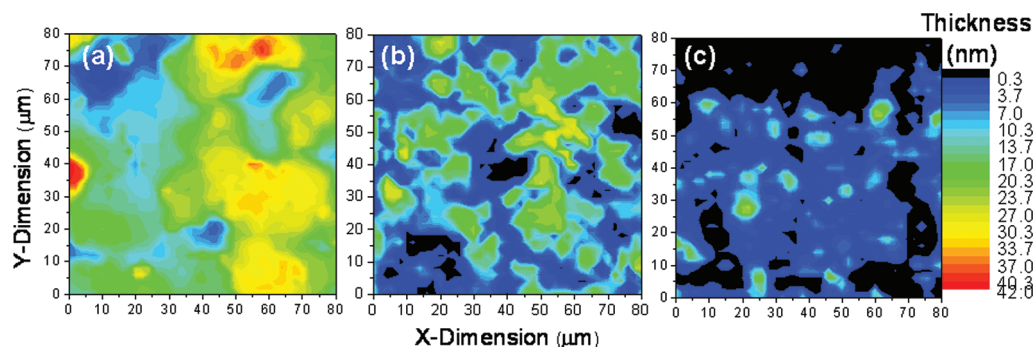


Figure 1. Spatial maps of the film thickness for (a) an as-grown EG film on SiC, (b) an EG film transferred using a 3 N/mm² bonding force onto a SiO₂ on Si handle substrate, and (c) the residual EG film remaining on SiC after the transfer process. The film thickness was measured using the method outlined in ref 24 and calibrated using AFM.

ited on sapphire substrates will be discussed, demonstrating that this process can be readily implemented for use with many handle substrates of interest. Transfer of EG from SiC has been performed using the exfoliation method,²¹ producing submicrometer-sized samples, which are not amenable to large-scale device manufacturing. A method for transferring large-area Si-face EG onto other substrates was reported by Unarunotai *et al.*²² during the review process of this paper that uses a peeling process; however, this effort produced devices with field effect mobilities of approximately 100 cm²/(V s) and relatively large Raman D line intensities, illustrating a substantial density of defects introduced during the transfer process. While a wet chemical approach has been successfully used to transfer metal-catalyzed graphene,^{10–12,23} this process is not amenable to EG on SiC, as SiC is highly resistant to chemical etchants. We report on Hall effect measurements and Raman spectroscopy that was performed on both as-grown and transferred EG films as well as fabricated devices from these films. The dry transfer process outlined here enabled the transfer of large-area (up to 16 mm on a side) and high-quality (relatively low Raman ‘D’ line intensities) EG films. Furthermore, devices subsequently fabricated in the transferred EG material exhibited Hall mobilities in excess of 1300 cm²/(V s), which was within 10% of the values measured in identical as-grown EG devices. Raman spectroscopy was also used to verify the thickness of the EG films and X-ray photoemission spectroscopy (XPS) measurements were performed to verify the transfer efficiency. In addition, the XPS characterization of the EG films during the transfer process revealed the presence of atomic silicon. These measurements indicate that this transfer process can enable large-area EG films on arbitrary substrates that are suitable for both device fabrication and further experiments exploring the influence of various substrates upon the electrical properties of the EG films.

RESULTS AND DISCUSSION

Presented in Figure 1 are two-dimensional Raman thickness maps, using the characterization technique

described in ref 24 for an (a) as-grown EG film on C-face 4H-SiC, (b) an EG film transferred using 3 N/mm² bonding force onto a SiO₂ on Si substrate, and (c) a residual EG film on C-face 4H-SiC following the successful removal of the upper EG layers. A schematic illustrating the transfer process is provided as Supporting Information. The map of the as-grown EG film (Figure 1a), indicates that there is considerable spatial variation in the initial film thickness, with the average thickness of this sample found to be approximately 19 nm, and typical values ranging from 10–30 nm. In comparison, the transferred EG films had average thicknesses ranging from 8–14 nm. However, similar spatial variations in the film thicknesses of the as-grown and transferred films were observed. Because the thickness variations observed before and after the EG transfer process were comparable, it was difficult to confirm if any changes in the thickness uniformity were induced *via* the transfer. It was also determined that the thickness of the residual EG layer on SiC following the transfer ranged from 0–5 nm in thickness, implying that about 90% of the EG film was removed *via* the transfer procedure, with subsequent XPS measurements verifying this transfer efficiency.

While the variations in the thickness uniformities of the as-grown and transferred EG films were similar, the transfer process created small voids in the transferred EG films. As shown in Figure 1b, voids on the order of 5–10 μm in size can be observed, which are not present in the as-grown films (Figure 1a). Regions of thick EG that are similar in size to the voids were observed in the residual EG on the SiC surface after the transfer process, as shown in Figure 1c. Presumably, the voids correlate to these local regions of thick residual EG. In addition, small regions where 10–20 nm reductions in the EG film thickness in the as-grown films were also observed. Therefore, it is possible that the voids in the transferred films are due to the inability of the transfer tape to make sufficient contact with the EG in these depressions, thereby leaving small areas of EG on the SiC surface after the transfer process. It should then be expected that the density and size of these voids will be reduced as advancements in EG growth leads to im-

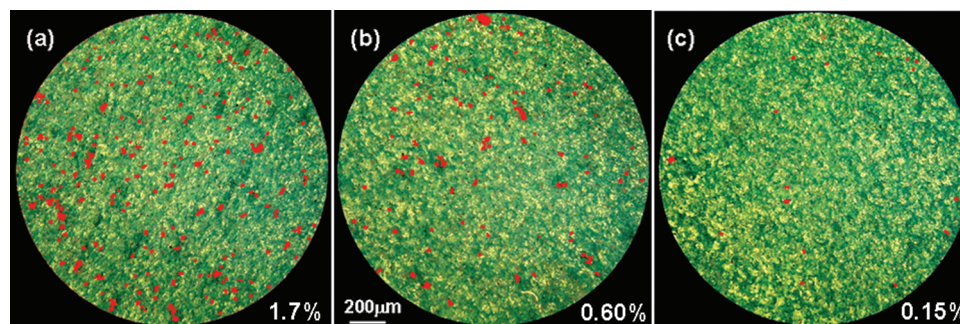


Figure 2. Nomarski micrographs of EG films transferred to SiO_2 on Si substrates following the application of (a) 3, (b) 4, and (c) 5 N/mm^2 force during the bonding of the thermal release tape to the EG on SiC prior to removal. Voids in the EG films have been highlighted in red for clarity and the percentage of the field-of-view where graphene is missing is reported in the lower left-hand corner of the images.

improvements in the thickness uniformity of the as-grown films.

To optimize the transfer process, a bonding force dependence study was performed. The force applied to the tape/EG/SiC stack was varied from 3–6 N/mm^2 , with a constant 3 N/mm^2 force applied during the second bonding step (tape/EG/handle substrate stack). Nomarski micrographs of the films transferred using 3, 4, and 5 N/mm^2 bonding forces were collected through a 10X, 0.25 NA objective and are presented in Figure 2a–c, respectively. These images illustrate that, as the force is increased from 3 to 5 N/mm^2 , the number of voids in the transferred EG films (highlighted in red in Figure 2a–c) are reduced. Therefore increasing the force during the tape to EG bonding stage leads to a more complete and continuous EG film. Subsequent particle analysis studies²⁵ were performed to measure

the percentage of the microscope field-of-view where EG was missing. The corresponding values are presented in Figure 2a–c. These measurements further illustrate the improvement in the transferred EG film continuity with increasing bonding force, as the areal percentage of voids was reduced 10-fold as the force was increased from 3 to 5 N/mm^2 . Presented in Figure 3a,b are μ -Raman spectra collected from the EG films transferred using 3 and 5 N/mm^2 bonding force, respectively. These spectra depict the relative intensities of the D ($\sim 1380 \text{ cm}^{-1}$), G ($\sim 1530 \text{ cm}^{-1}$) and 2D ($\sim 2700 \text{ cm}^{-1}$) Raman lines from selected areas with the highest (red trace) and lowest (blue trace) D:G intensity ratios (I_D/I_G). Previously, it was reported that this ratio varies inversely with the planar correlation length (approximate grain size) of the graphitic planes and may be used as a qualitative figure of merit for EG films,

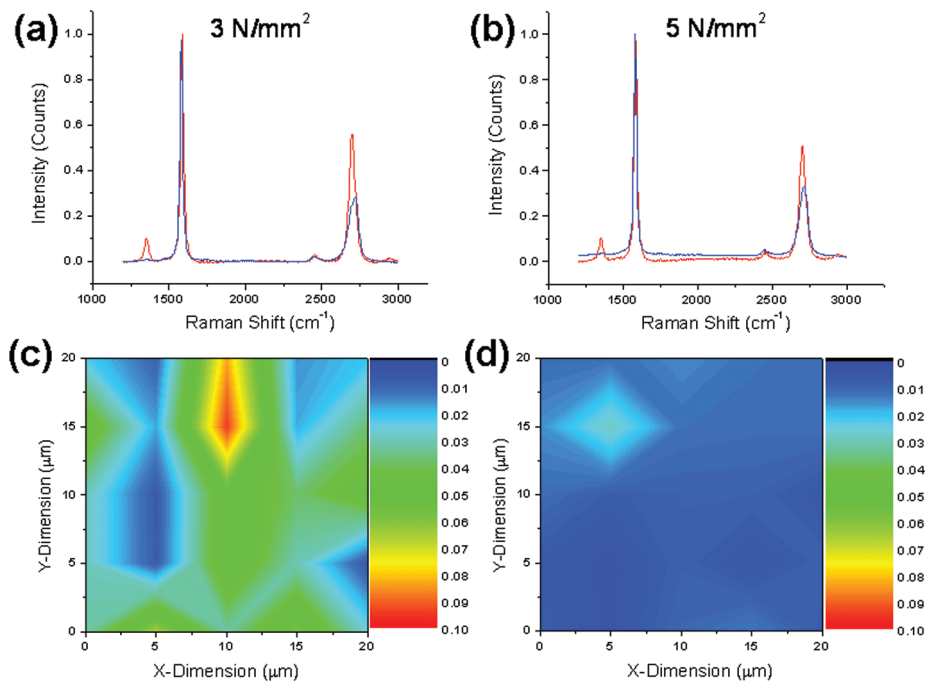


Figure 3. Micro-Raman spectra collected from EG films transferred to SiO_2 on Si substrates using a bonding force of (a) 3 and (b) 5 N/mm^2 . The spectra were collected from regions where there was high (red trace) and low (blue trace) intensities of the Raman D line. Corresponding maps representing the spatial distribution of the ratio of the Raman D to G intensities are presented in panels c and d, respectively.

with a low I_D/I_G indicating a higher quality graphene film.²⁶ Corresponding spatial maps of the I_D/I_G ratio over a $20\ \mu\text{m} \times 20\ \mu\text{m}$ area that are representative of these films are presented in Figure 3 panels c and d, respectively. A significant reduction in the I_D/I_G ratio was observed in films transferred using the higher bonding force, with average values of 0.037 ± 0.008 and 0.010 ± 0.002 being observed for films transferred using 3 and 5 N/mm^2 , respectively, with the error reported pertaining to the 95% confidence interval. This indicates further that a dramatic improvement in the material quality of the transferred EG films is induced with increasing bonding force. By comparison, I_D/I_G ratios of the as-grown EG films from the same wafer were found to range from 0.009 to 0.015, indicating that the optimized transfer process induced minimal additional degradation to the EG films outside of the regions where voids were present. Furthermore, the spatial uniformity of the I_D/I_G ratio was significantly increased in the film transferred using the higher bonding force. However, upon increasing the force to 6 N/mm^2 (not shown), only small islands of EG were removed and subsequently transferred. Therefore, this study indicates that a bonding force of approximately 5 N/mm^2 is optimal for enabling the transfer of continuous and uniform EG films with low defect densities from C-face SiC using this thermal release tape process. However, efforts involving graphene transfers from different growth substrates and/or using different adhesives may require further optimization. In subsequent experiments it was also determined that increasing the bonding force to the tape/EG/handle substrate stack to 5 N/mm^2 also improved the efficiency of the transfer of the EG films.

To determine the amenability of this transfer process to various other handle substrates, the optimized process described above, with the exception of the handle substrate surface preparation steps, was used to transfer EG films from C-face SiC onto p- and n-type GaN and also onto Al_2O_3 films deposited on c-face sapphire *via* atomic layer deposition (ALD). In the case of the former, the ALD Al_2O_3 film was required to modify the highly unreactive surface of the sapphire substrate to enable a successful transfer. Nomarski micrographs of these transferred EG films appeared very similar to EG transferred onto SiO_2 , therefore indicating that the transfer process is relatively insensitive to the handle substrate material.

To determine if any degradation to the electrical properties of the transferred films occurred during the transfer process, Hall measurements were initially performed on as-grown EG films and were repeated on EG films transferred to SiO_2 . Room temperature carrier mobilities from the $16\ \text{mm} \times 16\ \text{mm}$ and $10\ \text{mm} \times 10\ \text{mm}$ as-grown EG material ranged from 909 to 1875 $\text{cm}^2/(\text{V s})$, with an average mobility of 1485 $\text{cm}^2/(\text{V s})$ and an average carrier density of $15.8 \times 10^{13}\ \text{cm}^{-2}$ being observed. Following the transfer process, the mobil-

ity and carrier density from these large-area films both decreased significantly, with post-transfer mobility values ranging from 188 to 269 $\text{cm}^2/(\text{V s})$, with an average of 201 $\text{cm}^2/(\text{V s})$, while the carrier density reduced 3-fold to an average of $5.10 \times 10^{13}\ \text{cm}^{-2}$. Because this reduction in mobility was observed despite a corresponding decrease in carrier density, it is apparent that this mobility reduction is due to the introduction of additional scattering centers or defects, such as voids, within the EG films during the transfer process.

A large reduction in the carrier density in comparison to the values initially measured in the as-grown EG films was observed *via* the Hall effect following the transfer process. Sun *et al.*²⁷ showed that within a C-face EG film that there are graphene layers with varied levels of doping, proposing that the highest doped layers are located at or near the SiC–EG interface. As the transfer procedure discussed here removes all but the bottom most EG layers, the reduction in carrier density observed in the transferred EG films is consistent with the upper EG layers having a lower carrier density than those closest to the SiC interface. One would further expect that the residual EG films on SiC would exhibit a carrier density that was unchanged from the initial as-grown EG film measurements. However, due to a lack of electrical continuity of the post-transfer, residual EG films, Hall measurements were inconclusive. Interestingly, XPS measurements of multiple EG films bound to the thermal-release tape prior to transfer revealed the presence of a Si 2p peak at a binding energy of approximately 101 eV, implying that atomic Si is present within the EG layers. Subsequent measurements illustrated that the tape was not the source of this Si. Therefore, it is possible that these intercalated Si atoms are acting as an isoelectronic dopant and may account, at least in part, for the high sheet carrier densities found in EG in comparison to the reported intrinsic levels.^{28,29}

Since the spatial maps of the Raman I_D/I_G ratio indicated that minimal degradation to the EG film quality was induced *via* the transfer process over multiple 400 μm^2 regions, it is believed that the degradation in the carrier mobility is due mostly to the presence of voids in the films. Therefore, it would be expected that the observed degradation in the carrier mobility would be suppressed in smaller devices.¹⁹ To explore this possibility, 200 μm van der Pauw squares were lithographically patterned on both as-grown EG films and those transferred to SiO_2 on Si substrates using the optimized transfer process. The mobilities were found to improve to an average of 1348 $\text{cm}^2/(\text{V s})$ (range: 807–1800 $\text{cm}^2/(\text{V s})$), while an average mobility of 1476 $\text{cm}^2/(\text{V s})$ (range: 853–2200 $\text{cm}^2/(\text{V s})$) was recorded from the devices fabricated on the as-grown EG films. Furthermore, the carrier density was observed to reduce from $6.79 \times 10^{13}\ \text{cm}^{-2}$ (as-grown) to $3.18 \times 10^{13}\ \text{cm}^{-2}$ (transferred), similar to the reduction in carrier density observed *via* EG transfer in the large-area samples. In ad-

dition, the yield of the van der Pauw devices on the transferred EG films was nearly 100%, which further supports the notion that the voids make up less than 1% of the area of the transferred films, as shown in Figure 2c. It should be noted that these mobilities are 3–4 orders of magnitude higher than amorphous silicon and most flexible conductive films, such as organic thin film transistors.³⁰ Furthermore, the average sheet resistivity of these devices was found to be $R_s = 175 \Omega/\square$ for the transferred devices ($123 \Omega/\square$ for the as-grown devices), which although this is not as low as thin films of indium tin oxide,³¹ are similar to or better than those values reported for transferred graphene initially grown on Ni¹² and Cu²³ films. Similar measurements on large-area (1 cm²) EG films transferred to Al₂O₃ were found to also exhibit reasonable sheet resistivities ($R_s = 402 \Omega/\square$). However, as reported by Chen *et al.*,⁷ the intrinsic sheet resistance of graphene is expected to be as low as $30 \Omega/\square$, thus up to an order of magnitude reduction could be expected with further improvements to the as-grown EG films and/or transfer process.

CONCLUSIONS

In summary, we have presented a method enabling the dry transfer of large-area C-face EG films from SiC onto an arbitrary handle substrate, thereby greatly increasing the flexibility of graphene films for most electronic, optoelectronic, and mechanical applications. While we have focused most of this discussion on the

transfer of EG onto SiO₂ on Si substrates, successful transfers onto both p- and n-type MOCVD GaN and thin ALD-deposited Al₂O₃ films were also reported. Van der Pauw devices fabricated from EG films transferred onto SiO₂ *via* the optimized process were found to have carrier mobilities similar to those measured in devices fabricated on as-grown EG on SiC from the same wafer. In addition, the transferred films exhibited sheet resistivities on par or better than the values reported in transferred graphene layers originally grown on thin metal films,^{12,23} which is important if such films are to be used as transparent conductors. A large reduction in the carrier density was also observed following the EG transfer process, and the presence of atomic Si within the EG films was detected.

EG films transferred *via* this optimized process are amenable for use as optically transparent contacts for optoelectronic applications, although improvements in the thickness uniformity and reductions in the film thickness in C-face EG films would further enable this technology. In addition, the optimization of this or a similar process for the dry transfer of EG grown on Si-face SiC and/or metal-catalyzed graphene films would also be highly beneficial. However, in addition to the prescribed usage for optically transparent contacts, these films are also amenable for the fabrication of high performance flexible electronic devices³⁰ and for graphene device fabrication on dielectric substrates deemed most suitable for specific applications of interest.

METHODS

Epitaxial Graphene Growth and Preparation. EG was grown for these transfer experiments *via* the sublimation process on 2'' C-face 4H-SiC substrates that were previously chemically mechanically polished.^{18,19} The substrates were placed within an Aixtron/Epigress VP508 Hot-Wall chemical vapor deposition reactor and the surface was further prepared *via* an H₂ etch at 100 mbar and 1600 °C for 20 min. The chamber was evacuated to $(1.4-17) \times 10^{-4}$ mbar, and the temperature was lowered to 1550 °C for EG formation. EG growth was carried out for 1 h. After growth, the chamber was allowed to cool overnight.¹⁹ Square samples 10 mm on a side were cut from the 2'' C-face 4H-SiC substrate following EG growth, to enable multiple transfer attempts. For all measurements comparing the characteristics of transferred and as-grown EG films, adjacent samples from the same wafer were chosen. The SiO₂ on Si "handle" substrates used for the EG transfers consisted of 100 nm of thermally grown SiO₂ on n-type Si.

Graphene Transfer Process. To improve the bonding strength between the transferred EG and the SiO₂ surface, a cleaning and surface preparation procedure was used to produce a hydrophilic surface on the SiO₂. The SiO₂ surface was cleaned using a 750 W O₂ plasma treatment for 5 min in a Plasma-Preen II-973, followed by ultrasonic SC1 cleaning (5:1:1, H₂O:NH₄OH:H₂O₂) at 40 °C for 14 min, ending with a 1 min rinse in megasonic water provided by a Honda Electronics PulseJet (W-357–3MP) system at full power. Immediately before the transfer, the handle substrates were treated with a 30 s, 750 W O₂ plasma treatment, a 1 min ultrasonic SC1 clean and a 1 min megasonic rinse. With the exception of a standard solvent clean (isopropyl alcohol), the EG surface did not require any specific preparation procedures for a successful transfer. For the EG transfers to p- and n-type

GaN, 2 μm thick GaN films were grown on 2-in., a-plane sapphire substrates using metal organic chemical vapor deposition (MOCVD).³² The growth was initiated with a 25 nm AlN nucleation layer grown at 680 °C and 50 Torr with the subsequent GaN grown at 1025 °C and 50 Torr. The n- and p-type doping was accomplished with disilane and Cp₂Mg, respectively. EG films were also transferred onto 100 nm Al₂O₃ films grown *via* atomic layer deposition (ALD) on a 20 mm × 20 mm double-side polished, epi-grade, c-face sapphire substrate at a chamber temperature of 300 °C using tetramethyl aluminum and water as the alternating precursors. For the EG transfer to both GaN and Al₂O₃, the surface preparation of the handle substrate consisted of only a 5 min, 750 W O₂ plasma treatment in the Plasma Preen system.

Following the prescribed substrate pretreatment procedures, a precut piece of Nitto Denko Revalpha Thermal Release Tape (Part No. 3193MS, 7.3 N/mm) was placed on the EG surface. The tape/EG/SiC sample "stack" was then placed on a silicon wafer within the bore of an EVG EV501 wafer bonding apparatus. A 2'' stainless steel pressure plate was then placed on top of the stack to ensure a uniform force was applied. Following an evacuation of the bonding chamber to a pressure of approximately 5×10^{-4} Torr, a force between 3–6 N/mm² was applied to the stack for 5 min. After this process, the sample stack was removed from the bonder and the tape was peeled from the SiC wafer, thereby removing most of the EG layers from the SiC substrate. The tape with the removed EG layers was placed on the prepared SiO₂ on Si "handle" substrate and was then returned to the bonding apparatus, underneath the 2'' stainless steel pressure plate, where a force of 3–6 N/mm² was applied for 5 min. The stack was then removed and placed on a hot plate, where the surface temperature was stabilized at a temperature 1–2 °C above the 120 °C release temperature of the tape. This thermal treatment

eliminates the adhesion strength of the tape. The tape was then removed, leaving behind the transferred EG film on the handle substrate. The tape residue was dissolved using a solution of 1:1:1 toluene/methanol/acetone, and a final anneal at 250 °C for 10 min was performed to improve the transferred EG to SiO₂ adhesion. A schematic of this process is depicted in the Supporting Information section.

Micro-Raman Spectroscopic Setup. EG film thicknesses were estimated by measuring the attenuation of substrate Raman signal intensity (777 and 964 cm⁻¹ for EG on SiC; 521 cm⁻¹ for EG transferred to SiO₂ on Si) induced by the presence of the EG film.²⁴ Atomic force microscopy of various regions of interest was used to calibrate the attenuated Raman signal intensity to the measured EG film thickness, fitting the results to the following:

$$I = I_0 e^{-2\alpha d} \quad (1)$$

where I and I_0 represent the measured Raman intensity in the presence and absence of an EG film, respectively. The fitting parameter α corresponds to the relative extinction coefficient of the EG films on SiC, ($\alpha = 0.2 \text{ nm}^{-1}$) and of the EG and SiO₂ films on Si, ($\alpha = 0.0576 \text{ nm}^{-1}$). Raman measurements were performed confocally using either a 514.5 or a 532 nm laser line focused through a 100X, 0.9 N.A. or a 50X, 0.42 N.A. objective, respectively, in both cases providing a submicrometer laser spot with a power at the sample of approximately 10 mW. The collected signal was passed through an appropriate wavelength Semrock long-pass filter and was detected using either an Ocean Optics QE65000 CCD spectrometer or a half-meter Acton single spectrometer (SpectraPro-2500i) with a Princeton Instruments nitrogen-cooled, back-thinned, deep-depleted CCD array detector (SPEC-10:400BR/LN). Spatial mapping of the Raman peak characteristics (position, full-width at half max, center-of-mass, intensity and calculated EG film thickness) was achieved by translating the sample with respect to the laser spot.

Device Fabrication and Electrical Testing. To determine the effect of the transfer process on the electrical characteristics of the transferred EG films, Hall effect mobility and carrier density measurements were carried out at 300 K using a van der Pauw configuration. For 16 mm × 16 mm and 10 mm × 10 mm samples, beryllium–copper pressure clips were used as probe contacts to the corners of the as-grown and transferred films. For patterned 200 μm × 200 μm van der Pauw squares, standard probe manipulators were used as current and voltage leads to the gold contact pads. Measurement currents ranged from 1 to 100 μA while the magnetic field was approximately 2 kG.

Acknowledgment. We would like to thank Nitto Denko America (Fremont, CA), Electronics Process Material Group (system.nda@nitto.com) for providing the thermal release tape and expertise in the associated transfer and cleaning processes. Artwork for the table of contents figures was provided by M. Kraus (www.mammalcreative.com). The authors also express their appreciation to S. Binari for the use of his Hall effect measurement system and Je. Robinson and Jo. Robinson for helpful discussions. This work was supported in part by the Office of Naval Research. Support for J.L. Tedesco and J.K. Hite was provided by the ASEE.

Supporting Information Available: Schematic diagram of the transfer process. (a) The handle substrate is pretreated to improve surface bonding with the epitaxial graphene (EG) to be transferred. The procedure for SiO₂ on Si substrates is presented. (b) Thermal release tape is applied to the EG on SiC surface. (c) A uniform force is applied to tape/EG/SiC sample. (d) The tape is peeled from the SiC surface removing the majority of the EG film. (e) The tape and EG film are placed on the transfer substrate surface and a uniform force is once again applied to the tape/EG/substrate stack. (f) The stack is placed on a hot plate at a temperature 1–2° above the release temperature and the tape is removed. This material is available free of charge via the Internet at <http://pubs.acs.org>.

REFERENCES AND NOTES

- Novoselov, K. S.; Geim, A. K.; Morozov, S. V.; Jiang, D.; Zhang, Y.; Dubonos, S. V.; Grigorieva, I. V.; Firsov, A. A. Electric Field Effect in Atomically Thin Carbon Films. *Science* **2004**, *306*, 666–669.
- Avouris, P.; Chen, Z.; Perebeinos, V. Carbon-Based Electronics. *Nat. Nanotechnol.* **2007**, *2*, 605–613.
- Kuzmenko, A. B.; van Heumen, E.; Carbone, F.; van der Marel, D. Universal Optical Conductance of Graphite. *Phys. Rev. Lett.* **2008**, *100*, 117401.
- Nair, R. R.; Blake, P.; Grigorenko, A. N.; Novoselov, K. S.; Booth, T. J.; Stauber, T.; Peres, N. M. R.; Geim, A. K. Fine Structure Constant Defines Visual Transparency of Graphene. *Science* **2008**, *320*, 1308.
- Wang, X.; Linjie, Z.; Mullen, K. Transparent, Conductive Graphene Electrodes for Dye-Sensitized Solar Cells. *Nano Lett.* **2008**, *8*, 323–327.
- Lee, C.; Wei, X.; Kysar, J. W.; Hone, J. Measurement of the Elastic Properties and Intrinsic Strength of Monolayer Graphene. *Science* **2008**, *321*, 385–388.
- Chen, J. H.; Jang, C.; Xiao, S. D.; Ishigami, M.; Fuhrer, M. S. Intrinsic and Extrinsic Performance Limits of Graphene Devices on SiO₂. *Nat. Nanotechnol.* **2008**, *3*, 206–209.
- Jena, D.; Konar, A. Enhancement of Carrier Mobility in Semiconductor Nanostructures by Dielectric Engineering. *Phys. Rev. Lett.* **2007**, *98*, 136805.
- Konar, A.; Fang, T.; Jena, D. Effect of High-k Dielectrics on Charge Transport in Graphene. 2009, arXiv:0902.0819v1. arXiv.org e-Print archive. <http://adsabs.harvard.edu/abs/2009arXiv0902.0819K>. (Accessed December 5, 2009.)
- Yu, Q. K.; Lian, J.; Siriponglert, S.; Li, H.; Chen, Y. P.; Pei, S. S. Graphene Segregated on Ni Surfaces and Transferred to Insulators. *Appl. Phys. Lett.* **2008**, *93*, 113103.
- Reina, A.; Jia, X. T.; Ho, J.; Nezich, D.; Son, H. B.; Bulovic, V.; Dresselhaus, M. S.; Kong, J. Large Area, Few-Layer Graphene Films on Arbitrary Substrates by Chemical Vapor Deposition. *Nano Lett.* **2009**, *9*, 30–35.
- Kim, K. S.; Zhao, Y.; Jang, H.; Lee, S. Y.; Kim, J. M.; Kim, K. S.; Ahn, J. H.; Kim, P.; Choi, J. Y.; Hong, B. H. Large-Scale Pattern Growth of Graphene Films for Stretchable Transparent Electrodes. *Nature* **2009**, *457*, 706–710.
- Li, X. S.; Cai, W. W.; An, J. H.; Kim, S.; Nah, J.; Yang, D. X.; Piner, R.; Velamakanni, A.; Jung, I.; Tutuc, E.; et al. Large-Area Synthesis of High-Quality and Uniform Graphene Films on Copper Foils. *Science* **2009**, *324*, 1312–1314.
- Berger, C.; Song, Z. M.; Li, T. B.; Li, X. B.; Ogbazghi, A. Y.; Feng, R.; Dai, Z. T.; Marchenkov, A. N.; Conrad, E. H.; First, P. N. Ultrathin Epitaxial Graphite: 2D Electron Gas Properties and a Route Toward Graphene-Based Nanoelectronics. *J. Phys. Chem. B* **2004**, *108*, 19912–19916.
- Forbeaux, I.; Themlin, J. M.; Debever, J. M. Heteroepitaxial Graphite on 6H-SiC(0001): Interface Formation Through Conduction-Band Electronic Structure. *Phys. Rev. B* **1998**, *58*, 16396.
- Charrier, A.; Coati, A.; Argunova, T. Solid-State Decomposition of Silicon Carbide for Growing Ultra-Thin Heteroepitaxial Graphite Films. *J. Appl. Phys.* **2002**, *92*, 2479–2484.
- Gaskill, D. K.; Jernigan, G.; Campbell, P.; Tedesco, J. L. Epitaxial Graphene Growth on SiC Wafers. *ECS Trans.* **2009**, *19*, 117–124.
- Jernigan, G. G.; vanMil, B. L.; Tedesco, J. L.; Tischler, J. G.; Glaser, E. R.; Davidson, A.; Campbell, P. M.; Gaskill, D. K. Comparison of Epitaxial Graphene on Si-face and C-face 4H-SiC Formed by Ultrahigh Vacuum and RF Furnace Production. *Nano Lett.* **2009**, *9*, 2605–2609.
- VanMil, B. L.; Myers-Ward, R. L.; Tedesco, J. L.; Eddy, C. R.; Jernigan, G. G.; Culbertson, J. C.; Campbell, P. M.; McCrate, J. M.; Kitt, S. A.; Gaskill, D. K. Graphene Formation on SiC Substrates. *Mater. Sci. Forum* **2009**, *615–617*, 211–214.
- Tedesco, J. L.; vanMil, B. L.; Myers-Ward, R. L.; McCrate, J. M.; Kitt, S. A.; Campbell, P. M.; Jernigan, G. G.; Culbertson,

- J. C.; Eddy, C. R.; Gaskill, D. K. Hall Effect Mobility of Epitaxial Graphene Grown on Silicon Carbide. *Appl. Phys. Lett.* **2009**, *95*, 122102.
21. Lee, D. S.; Riedl, C.; Krauss, B.; von Klitzing, K.; Starke, U.; Smet, J. H. Raman Spectra of Epitaxial Graphene on SiC and of Epitaxial Graphene Transferred to SiO₂. *Nano Lett.* **2008**, *8*, 4320–4325.
22. Unarunotai, S.; Murata, Y.; Chialvo, C. E.; Kim, H.-s.; MacLaren, S.; Mason, N.; Petrov, I.; Rogers, J. A. Transfer of Graphene Layers Grown on SiC Wafers to Other Substrates and Their Integration into Field Effect Transistors. *Appl. Phys. Lett.* **2009**, *95*, 202101.
23. Li, X.; Zhu, Y.; Cai, W.; Borysiak, M.; Han, B.; Chen, D.; Piner, R. D.; Colombo, L.; Ruoff, R. S. Transfer of Large-Area Graphene Films for High-Performance Transparent Conductive Electrodes. *Nano Lett.* **2009**, *9*, 4359–4363.
24. Shivaraman, S.; Chandrashekhar, M.; Boeckl, J. J.; Spencer, M. G. Thickness Estimation of Epitaxial Graphene on SiC using Attenuation of Substrate Raman Intensity. *J. Electron. Mater.* **2009**, *38*, 725–730.
25. Rasband, W. ImageJ 1.38x, <http://rsb.info.nih.gov/ij/>. (Accessed February 1, 2009.)
26. Tuinstra, F.; Koenig, J. L. Raman Spectrum of Graphite. *J. Chem. Phys.* **1970**, *53*, 1126–1130.
27. Sun, D.; Wu, Z.-K.; Divin, C.; Li, X.; Berger, C.; De Heer, W. A.; First, P. N.; Norris, T. B. Ultrafast Relaxation of Excited Dirac Fermions in Epitaxial Graphene Using Optical Differential Transmission Spectroscopy. *Phys. Rev. Lett.* **2008**, *101*, 157402.
28. Dawlaty, J. M.; Shivaraman, S.; Chandrashekhar, M.; Rana, F.; Spencer, M. G. Measurement of Ultrafast Carrier Dynamics in Epitaxial Graphene. *Appl. Phys. Lett.* **2008**, *92*, 042116.
29. Fang, T.; Konar, A.; Xing, H. L.; Jena, D. Carrier Statistics and Quantum Capacitance of Graphene Sheets and Ribbons. *Appl. Phys. Lett.* **2007**, *91*, 092109.
30. Mas-Torrent, M.; Rovira, C. Novel Small Molecules for Organic Field-Effect Transistors: Towards Processability and High Performance. *Chem. Soc. Rev.* **2008**, *37*, 827–838.
31. Kim, H.; Horwitz, J. S.; Kushto, G. P.; Kafafi, Z. H.; Chrisey, D. B. Indium Tin Oxide Thin Films Grown on Flexible Plastic Substrates by Pulsed-Laser Deposition for Organic Light-Emitting Diodes. *Appl. Phys. Lett.* **2001**, *79*, 284–286.
32. Eddy, C. R.; Holm, R. T.; Henry, R. L.; Culbertson, J. C.; Twigg, M. E. Investigation of Three-Step Epilayer Growth Approach of GaN Films to Minimize Compensation. *J. Electron. Mater.* **2005**, *34*, 1187–1192.